Available online at www.sciencedirect.com
ScienceDirect
Ceramics International 38 (2012) 277–282
CERAMICS INTERNATIONAL
www.elsevier.com/locate/ceramint

Modified $Pb(Yb,Nb)O_3$–$PbZrO_3$–$PbTiO_3$ ternary system for high temperature applications

Jong Bong Lim [a,*], Shujun Zhang [b], Thomas R. Shrout [b]

[a] *Nano. Functional Materials Group, Korea Institute of Materials Science, Changwon, Gyeongnam 641-831, Republic of Korea*
[b] *Material Research Institute, Pennsylvania State University, University Park, State College, PA 16802, USA*

Received 2 April 2011; received in revised form 4 July 2011; accepted 5 July 2011
Available online 18th July 2011

Abstract

Ternary $33Pb(Yb_{1/2}Nb_{1/2})O$–$(67-x)PbZrO_3$–$xPbTiO_3$ [PYNZ–PTx] were investigated as a function of the PT contents. The maximum value of piezoelectric coefficient (d_{33}) was obtained, being on the order of 540 pm/V with high Curie temperature (Tc) of 375 °C for PYNZ–PT48 composition being regarded as the morphotropic phase boundary (MPB). To further increase its properties, La_2O_3 with 0.0 mol% $\leq x \leq$ 3.0 mol% was substituted for PbO as an A-site in ternary PYNZ–PT48 [PYNZT]. The substitution of La^{3+} for Pb^{2+} in PYNZT was found to increase the tetragonality, but greatly reduced Tc and broadened the dielectric permittivity maximum. The relative permittivity was found to follow a Curie–Weiss Law above the deviation temperature (T_D). The optimized properties with d_{33} of 600 pm/V, maximum dielectric permittivity (ε_{max}) of 22500 (at the Tc = 315 °C and 1 kHz) were obtained in PYNZT-La2.0.

Keywords: PYN-PZ-PT; Curie–Weiss; Phase transition; High-Tc

1. Introduction

In recent years, ferroelectric relaxor-based perovskite compounds $Pb(B_1,B_2)O_3$ have been widely used in harsh temperature applications, such as actuators, high signal acoustic transducers and small signal sensor [1,2]. In such applications of piezoelectric devices, ferroelectric relaxor materials should possess not only high Curie temperature (Tc), but also excellent piezoelectric properties because relaxor piezoelectric materials with high Tc can offer an extended operating temperature range with temperature stability in their electrical performance [3].

Since Smolenskii and Agranovkaya [4] first introduced complex perovskites with the dielectric properties and phase transformation behavior, much attention has focused on ternary system, for example $Pb(Mg,Nb)O_3$–$PbZrO_3$–$PbTiO_3$ [5] and $Pb(Mg,Ta)O_3$–$PbZrO_3$–$PbTiO_3$ [6]. Ternary $[(1-x)Pb(Yb,Nb)O_3$–$xPbTiO_3]$–$PbZrO_3$ [PYN–PT–PZ] was firstly reported by Im and Choo [7] that the crystal structure was changed sequentially from the pseudocubic to rhombohedral or tetragonal phase with relaxor behavior, but no information on the piezoelectric properties was described. Ohuchi et al. [8] investigated xPYN–yPT–zPZ as well as the existence in a morphotropic phase boundary (MPB) region showing anomalously high dielectric and piezoelectric properties, but they have reported few piezoelectric properties with phase transformation. Yoon et al. [9,10] reported PYN-PZ-PT with improvement of electromechanical coupling factor (k_p) and mechanical quality factor (Q_m). However, the improved piezoelectric properties near the MPB region with high Tc are still unsatisfied for practical use. Recently, Zhu and Ye [11] systematically investigated and reported a ternary PYN-PZ-PT system with high Tc of 370 °C and excellent d_{33} of 1247 pC/N at 20 kV/cm, which make it further challenges as a promising candidate for high temperature application. To accomplish higher dielectric and piezoelectric activity, MPB-based PYN-PZ-PT systems are required to be further engineered by compositional adjustment through the addition of donor dopants into A or B site, which leads to a structure change and the downward shift of the phase transition temperature for PYN-PZ-PT. As one of donor dopants, La_2O_3 is well known to decrease both the phase transition temperature and oxygen vacancy concentration, which leads to further improving dielectric and piezoelectric properties.

* Corresponding author. Tel.: +82 55 280 3594; fax: +82 55 280 3289.
E-mail address: limjongbong@gmail.com (J.B. Lim).

0272-8842/$36.00
doi:10.1016/j.ceramint.2011.07.003

According to our previous study of ternary $(1-x-y)$PYN–xPZ–yPT, working along the line of MPB curve in the phase diagram of ternary PYN-PZ-PT [8], we have tried to develop high strain ($d_{33} \geq 500$ pC/N) and high coupling factor ($k_{33} \geq 60\%$) piezoelectrics with high Tc($\geq$300 °C) for multilayer actuators and ultrasonic transducers, resulting in optimum composition of 33PYN–23PZ–44PT satisfying requirements. However, MPB-based PYN–PZ–PT systems are required to be further engineered by compositional adjustment to accomplish higher piezoelectric activity. Based on our previous work, in this work, 33PYN–$(67-x)$PZ–xPT system was tuned up by adjusting the ratio of PZ to PT and characterized to find the MPB composition. In order to further optimize the piezoelectric properties of PYNZ–PTx, La_2O_3 was substituted for PbO as an A-site in PYNZ–PTx and its effect of La_2O_3 on the structural change and relaxor behavior of frequency dependency was characterized.

2. Experimental procedure

Conventional mixed oxide processing was used to prepare the $33Pb(Yb_{1/2}Nb_{1/2})O_3$–$(67-x)PbZrO_3$–$xPbTiO_3$ [PYNZ–PTx] with $44 \leq x \leq 50$. Samples were fabricated with high-purity oxide powders: Pb_3O_4 (99.9%, MCP Inc.), Yb_2O_3 (99.9%, PIDC), Nb_2O_5 (99.9%, Ferro), TiO_2 (99.9%, Aldrich Chemical), and ZrO_2 (99.5%, Ferro). $YbNbO_4$ was first prepared at 1200 °C for 4 h prior to reaction with PbO using the columbite precursor method [12] in a PYNZ–PTx formation. The PYNZ–PTx powders were stoichiometrically weighed and mixed for 24 h using ball milling in an anhydrous ethanol solution with stabilized zirconia media. These mixtures were then dried and calcined at 800 °C for 3 h to form the desired perovskite phase. In addition, La_2O_3 (99.9%, Aldrich Chemical) with 0.0 mol% $\leq x \leq$ 3.0 mol% was added into the optimized PYNZ–PTx composition to further improve their properties. The calcined powders were then vibratory-milled again with an acrylic binder. After debinding at 550 °C for 4 h, all samples were embedded in the source powder of the same composition to minimize the loss of PbO during the sintering and sintered at 1220 °C for 2 h in a closed crucible, resulting in theoretical density of >96%. Sintered samples were poled for 15 min at 150 °C under 30 kV/cm, subsequently cooled down to room temperature with maintaining the same electric filed.

The crystal structures and lattice parameters were identified by X-ray powder diffraction (XRD; PAD V diffractometer, Scintag Inc., Cupertino, CA) and the microstructure of the sintered samples was observed using scanning electron microscopy (SEM; S-3500N, Hitachi), respectively. The density for all samples was measured by the Archimedes method, exhibiting approximately 96% of theoretical density. The dielectric permittivity and dielectric loss were determined using a multifrequency LCR meter (HP4284A, Hewlett-Packard, Palo Alto, CA) over a temperature range of RT ~ 400 °C in a computer-controlled furnace. The polarization-electric field hysteresis (P–E) loops were measured using a modified Sawyer-Tower circuit driven at a field of 20 kV/cm supplied by a high-voltage power supply (TREK Model 610, TREK, Median, NY).

3. Results and discussion

Fig. 1 shows X-ray diffraction patterns for the PYNZ–PTx with $44 \leq x \leq 50$ sintered at 1220 °C for 2 h. All XRD patterns indicated a perovskite structure, and only a trace amount of pyrochlore phase was developed over the entire range of the solid solution system, probably by the evaporation of PbO during the sintering. The change in the peak split related to the structural phase transition was confirmed in PYNZ–PTx with different amounts of x ($PbTiO_3$). As shown in Fig. 1(a) for PYNZ–PT44, all peaks were indexed as a rhombohedral phase. With increasing the amount of x, however, the peak for (2 0 0) at $2\theta = 44.2°$ started splitting into two peaks of (0 0 2) and (2 0 0), and its intensity increased as well; indicating that a rhombohedral phase was changed to a tetragonal one, as shown in Fig. 1(b)–(d). In addition, the lattice constants and tetragonality (c/a) for PYNZ–PTx are listed in Table 1. As shown, with the increase in the amount of x, the a-axis was gradually decreased, whereas the c-axis was slightly increased. The tetragonality was observed to linearly increase as well, showing the similar tendency to the c-axis because of PT having the high degree of tetragonality.

The temperature dependence of the dielectric permittivity for PYNZ–PTx was measured at 1 MHz, as shown in Fig. 2. Above room temperature, ternary PYNZ–PTx normally exhibited only a peak for the phase transition temperature (Tc) corresponding to rhombohedral to cubic or tetragonal to cubic as a function of x, respectively, caused by the structural change as a function of various amounts of x in Fig. 1. The value of Tc in Fig. 2 was increased from 355 °C to 385 °C by increasing amounts of x, exhibiting the linear variation in Tc against x. As shown, increasing the amount of x increased Tc by about 5 °C/mol% because of $PbTiO_3$ having high Tc (~490 °C). The inset in Fig. 2 shows the dielectric permittivity for PYNZ–PT48 with various frequencies (0.1 kHz ~ 1.0 MHz). With the increase of

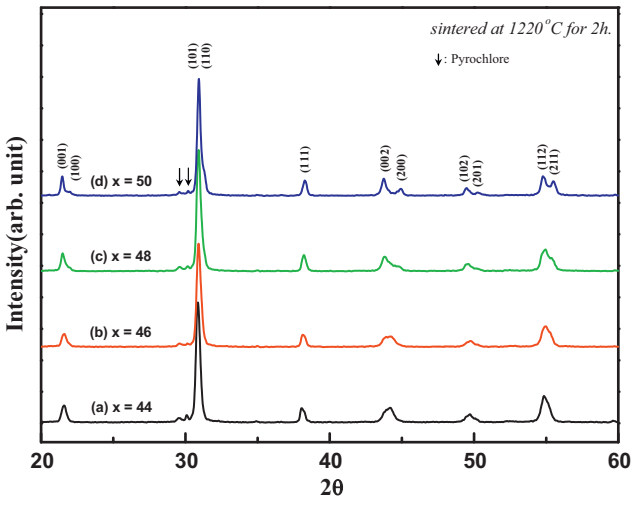

Fig. 1. XRD patterns of PYNZ–PTx with (a) x = 44, (b) x = 46, (c) x = 48, and (d) x = 50.

Table 1
Detailed piezoelectric properties and lattice constants for PYNZ–PTx with $44 \leq x \leq 50$ at 1 kHz.

PYN	PZ	PT	Tc (°C)	d_{33} (pm/V)	ε_r	tan δ	Lattice constant (A°)		c/a
							a_T	c_T	
33	23	44	355	420	720	0.024	4.0947	4.1178	1.0056
33	21	46	370	450	869	0.021	4.0895	4.1195	1.0073
33	19	48	375	540	1705	0.020	4.0513	4.1303	1.0195
33	17	50	385	510	1527	0.015	4.0307	4.1357	1.0260

frequencies, it exhibited typical ferroelectric behavior with a sharp peak for the phase transition from tetragonal to cubic at high temperature.

Fig. 3 shows the strain for unipolar curves and hysteresis loops for PYNZ–PTx measured at 20 kV/cm. As shown in Fig. 3(a), it revealed that the unipolar strain was increased with increase of x, and its variation with applied electric field was observed to be basically linear. In addition, the piezoelectric coefficient d_{33} calculated from the slope of the unipolar strain curve was found to be high, being on the order of 540 pm/V for PYNZ–PT48, which probably due to the ease of multi-domains reversal and polarization switching arising from the coexistence of the rhombohedral and tetragonal phases near at MPB. Fig. 3(b) shows the P–E hysteresis loops against the applied electric field. As shown, it was found that both the remnant polarization (P_r) and coercive field (E_c) were observed to be small variation with the increase of x, but was not significant. According to the above results, it can be considered that ternary PYNZ–PT48 exhibiting the maximum values for both the strain and P_r should be close to MPB composition. The detailed properties of PYNZ–PTx with $44 \leq x \leq 50$ are summarized in Table 1.

To further improve their properties for ternary PYNZ–PTx, La_2O_3 was substituted for PbO in PYNZ–PT48 to induce the downward shift in Curie temperature. Fig. 4 shows X-ray diffraction patterns of PYNZ–PT48 + x La_2O_3 [PYNZT-Lax] with 0.0 mol% $\leq x \leq$ 3.0 mol%. As shown in Fig. 4(a), pure PYNZT was found to be tetragonal phase, and its intensity was increased as the addition of La_2O_3, indicating the increase of tetragonality, shown in Fig. 4(b)–(e). Pyrochlore as a secondary phase was also observed in all compositions, which is related to Pb-deficient Yb/Nb mixed compound [9]. The lattice constants and tetragonality for PYNZT-Lax are listed in Table 3. With increasing the amount of La_2O_3, the a-axis was slightly decreased, while both the c-axis and tetragonality were increased, but not significant. According to the above results, it could be considered that the La^{3+} roles as a donor dopant and makes the switching of the domain easer, effectively domain walls. In addition, the addition of La^{3+} stabilized the tetragonal phase in PYNZT system.

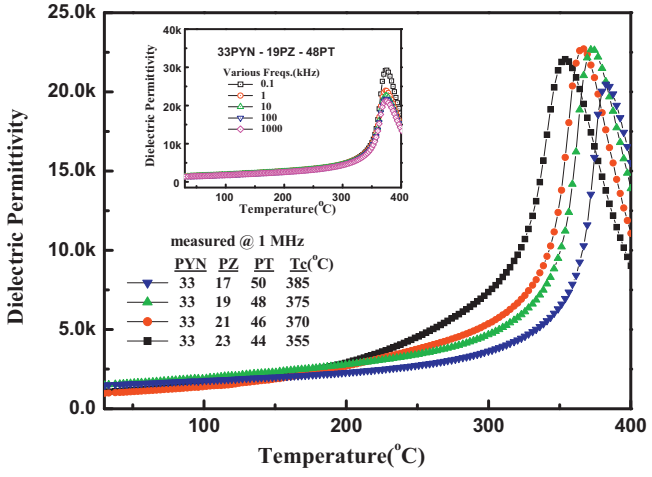

Fig. 2. Temperature dependence of dielectric permittivity for PYNZ–PTx. The inset shows the relative permittivity for PYNZ–PT48 against various frequencies.

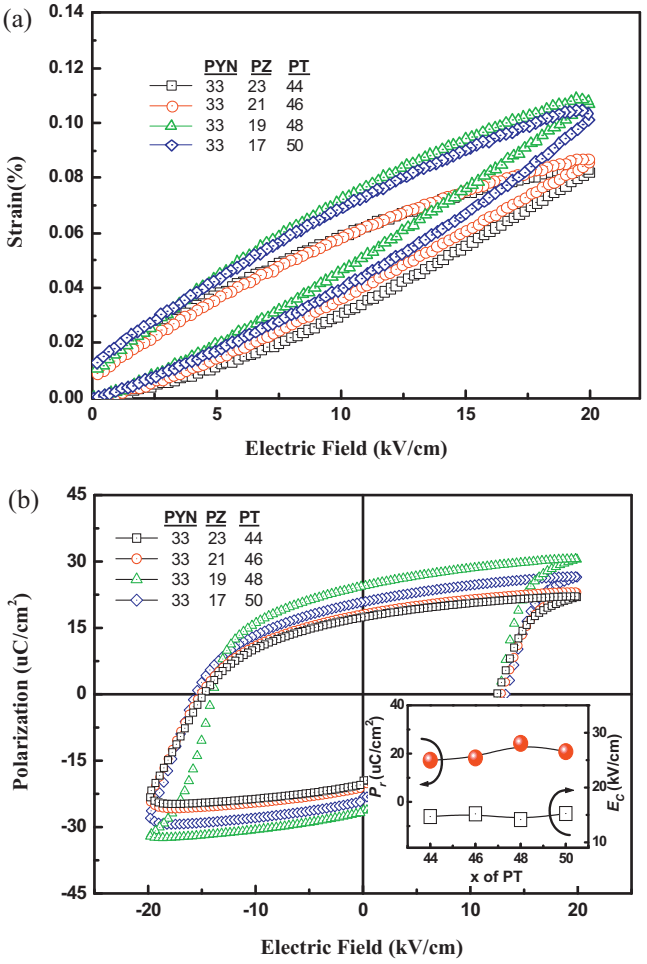

Fig. 3. (a) Unipolar strain curves and (b) P–E loops for PYNZ–PTx measured at 20 kV/cm.

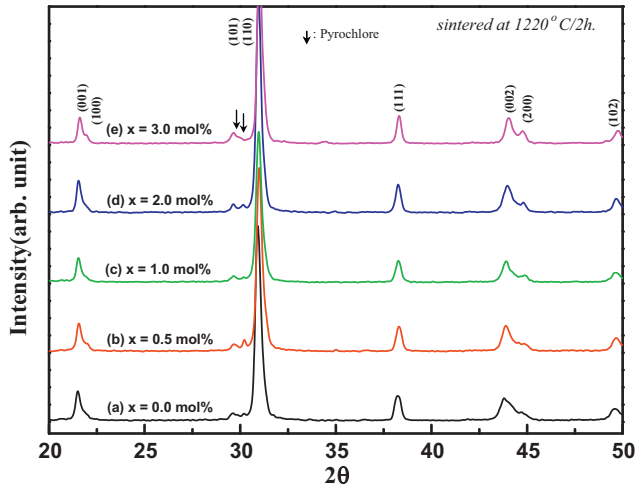

Fig. 4. XRD patterns of PYNZT-Lax with (a) $x = 0.0$ mol%, (b) $x = 0.5$ mol%, (c) $x = 1.0$ mol%, (d) $x = 2.0$ mol% and (e) $x = 3.0$ mol% sintered at 1220 °C for 2 h.

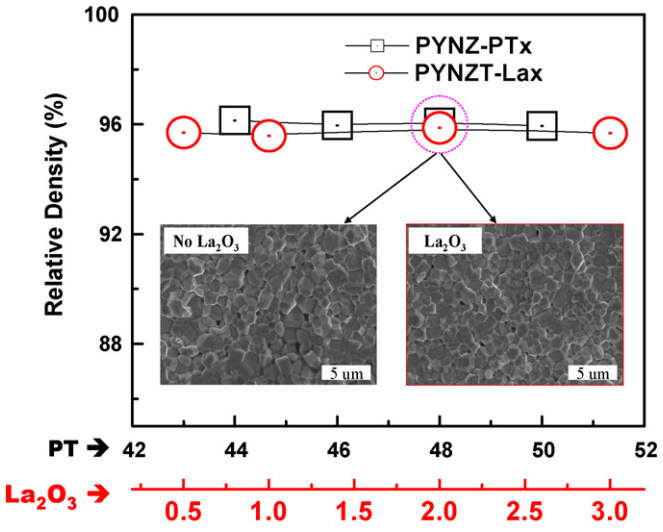

Fig. 5. Relative density and microstructure of PYNZT-Lax, compared to that of PYNZ–PTx.

Fig. 5 shows relative density and microstructure of PYNZT-Lax, compared to that of PYNZ–PTx, respectively. Relative density for pure PYNZ–PTx was found to be high with approximately 96% and its variation was not significant as a function of PT. When La^{3+} was substituted for Pb^{2+}, relative density of La-doped PYNZT was found to be a little bit lower than those of pure PYNZ–PTx, but was also still high with no variation. In the case of microstructures for PYNZ–PT48 with and without La_2O_3 (see the inset of Fig. 5), it could be observed that both the samples formed dense microstructures, but the grain size for pure sample seemed to be larger than those for La-doped sample, but not big different. Therefore, it can be considered that the microstructures as well as the relative densities for ternary PYN-PZ-PT system were not strongly affected by the addition of La_2O_3, leading to no big difference for both the samples.

Fig. 6 illustrates the dielectric permittivity of PYNZT-Lax as a function of temperatures. For pure PYNZT, the value of Tc was found at 375 °C with a narrow peak. As the amount of x was increased, the value of Tc was decreased from 375 °C to 290 °C by about 28.3 °C/mol%La_2O_3, and its transition range was found to become broader, indicating typical relaxor ferroelectric behavior caused by the randomly oriented polar micro-regions originated from compositional fluctuations on the nanometer length scale [13]. Furthermore, when La^{3+} substituted Pb^{2+} in PYNZT, La^{3+} acts as a donor, which reduce oxygen vacancy concentration ($La_2O_3 \overset{PYNZT}{\longrightarrow} 2La_{Pb}^{\bullet} + O_O$), resulting in making the domain re-alignment easy and increasing the dielectric constant [14]. Therefore, it can be considered that the addition of x increased the tetragonality at room temperature, which causes the Tc to shift downward in PYNZT, resulting in further improvement of dielectric and piezoelectric properties. The inset in Fig. 6 shows temperature dependences of the inverse relative permittivity for PYNZT-La3.0. In order to avoid space–charge polarization contributions at high temperatures and lower measurement frequency, the 1 MHz data is presented in the inset of Fig. 6. As shown, the inverse relative permittivity of PYNZT-La3.0 against temperature followed a Curie–Weiss Law above the deviation temperature (T_D), but exhibited large deviation below T_D. The diffuseness of the permittivity maxima can be described by an

Table 2
Summary of the ε_{max}, T_{max}, δ, and γ values for PYNZT-Lax with 0.0 mol% $\leq x \leq$ 3.0 mol% at 1 MHz.

Composition	ε_{max}	T_{max} (°C)	Diffuseness parameters		
			δ (°)	γ	C ($\times 10^5$ °C)
PYNZT-La0.0	29,300	376	15.08	1.03	36.88
PYNZT-La0.5	23,500	368	24.27	1.09	38.51
PYNZT-La1.0	23,000	358	23.43	1.32	66.07
PYNZT-La2.0	22,500	324	25.14	1.58	80.83
PYNZT-La3.0	21,400	311	26.27	1.61	92.06

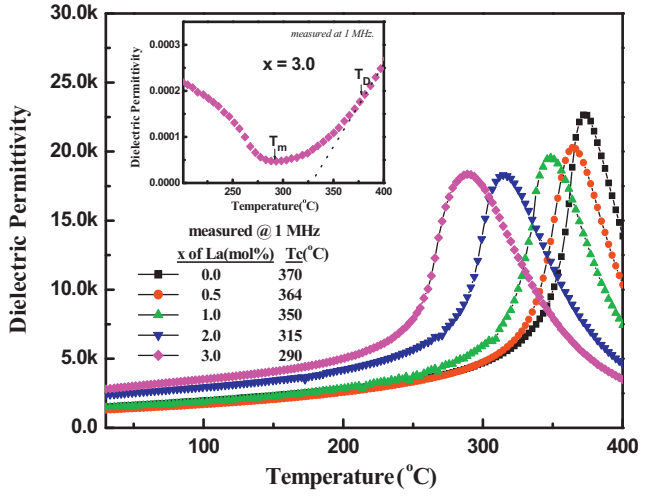

Fig. 6. Temperature dependence of dielectric permittivity for PYNZT-Lax. The inset shows the inverse relative permittivity for PYNZT-La3.0 against temperatures.

empirical expression previously developed by Smolenskii and Kirillov [15,16] as

$$\frac{1}{\varepsilon_r^T} - \frac{1}{\varepsilon_{max}} = \frac{(T_D - T_{max})^\gamma}{2\varepsilon_{max}\delta^\gamma}$$

where ε_r^T is permittivity, ε_{max} is the permittivity at T_{max}, T_D is deviation temperature from the Curie–Weiss behavior, δ is the diffuse parameter describing the width of the diffuse phase transition, and γ is the critical exponent that varies from $\gamma = 1$ for a purely normal ferroelectric to $\gamma = 2$ for a purely relaxor ferroelectric [17]. In addition, Curie constant (C) corresponding to high temperature paraelectric phase driven by a displacive transition with $C \sim 10^5$ °C and by the order–disorder transition with $C \sim 10^3$ °C [18] was calculated from a log–log plot of $[1/\varepsilon_r - 1/\varepsilon_{max}]$ vs. $[T - T_{max}]$. At the high temperature region, it was observed that the inverse permittivity for a PYNZT-La0.0 followed C–W behavior from 400 °C to T_D (375 °C) with the diffuseness parameters of $\gamma = 1.03$, $\delta = 15.08°$ and Curie constant of 36.88×10^5 °C. With increasing the content of Lax, the value of γ was found to be gradually increased up to 1.61 for PYNZT-La3.0, indicating a transition from normal to relaxor ferroelectrics. Furthermore, even though Curie constants were revealed to increase linearly, all Curie constants in PYNZT-Lax system were found to be $\sim 10^5$ °C, resulting in typical of displacive based transition at high temperature paraelectric phase. In the case of the diffuse parameter (δ), it was observed to be increased with increasing the contents of Lax, but not significant. From the above results, therefore, it can be suggested that the increase in the amount of Lax leads PYNZT to induction of a soft optic mode condensation or a displacive transition [19]. Detailed ε_{max}, T_{max}, and diffuseness parameters for PYNZT-Lax with 0.0 mol% $\leq x \leq$ 3.0 mol% are summarized in Table 2, which are similar to PZN [17] and PMN [20], respectively.

Unipolar strain curves and *P–E* hysteresis loops of PYNZT measured at 20 kV/cm as a function of the content of x are shown in Fig. 7. Strain measurements in strain indicated that there are considerable composition dependences within the range of a few contents of x, as shown in Fig. 7(a). Nonlinearity in strain hysteresis is generally related to domain switching which is creating the transient domain wall as a major source of strain under high electric field conditions [21]. The piezoelectric coefficient d_{33} exhibited the maximum of 600 pm/V at $x = 2.0$ mol%La_2O_3. As shown in the inset of Fig. 7(a), the

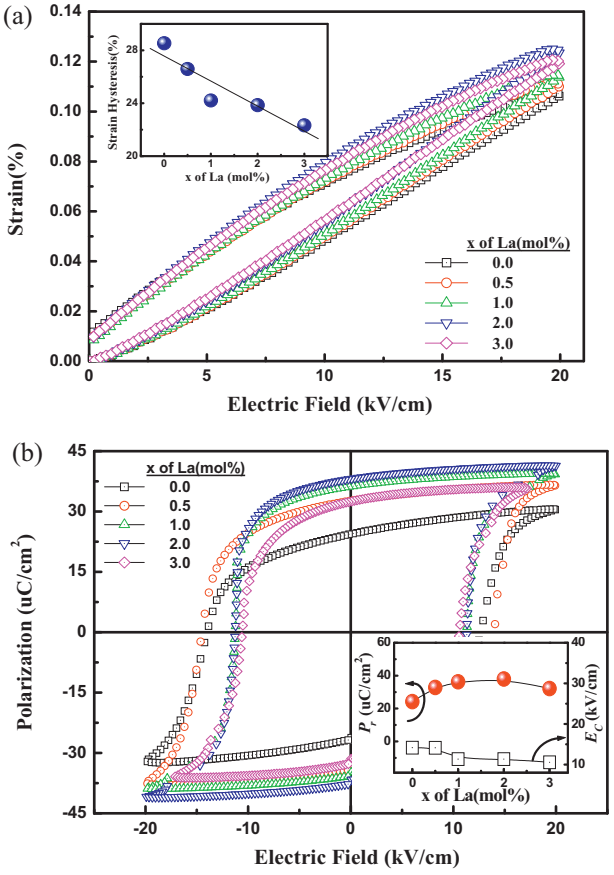

Fig. 7. (a) Unipolar strain curves and (b) *P–E* loops for PYNZT-Lax measured at 20 kV/cm. The insets are for strain hysteresis from (a) and for *Pr* and *Ec* from (b), respectively.

variation of strain hysteresis was linearly decreased with increasing amount of x due to the increase in tetragonality. Fig. 7(b) shows that the *P–E* hysteresis loops of the samples revealed well-defined square-like hysteresis loops. With increasing the content of x, the P_r was slightly increased and maximized at $x = 2.0$ mol%La_2O_3, whereas the *Ec* was found to be gradually decreased. Thus, it can be considered that these results might be due to the increase in the tetragonality and the degree of oxygen octahedral tilting for PYNZT. The detailed properties of PYNZT-Lax with 0.0 mol% $\leq x \leq$ 3.0 mol% are summarized in Table 3.

Table 3
Detailed piezoelectric properties and lattice constants for PYNZT-Lax with 0.0 mol% $\leq x \leq$ 3.0 mol% at 1 kHz.

x	Tc	d_{33}	ε_r	tan δ	Lattice constant (A°)		c/a
(mol%)	(°C)	(pm/V)			a_T	c_T	
0.0	375	540	1700	0.020	4.0513	4.1303	1.0195
0.5	364	545	1880	0.020	4.0508	4.1310	1.0197
1.0	350	575	1990	0.020	4.0498	4.1315	1.0201
2.0	315	600	2490	0.021	4.0487	4.1332	1.0208
3.0	290	585	2920	0.022	4.0461	4.1339	1.0216

4. Summary

Solid solution ternary PYNZ–PTx and La-doped PYNZ–PTx were synthesized using conventional method. Firstly, PYNZ–PTx compositions with $44 \leq x \leq 50$ were characterized against various temperatures and applied electric fields. The optimum composition of PYNZ–PT48 near the MPB region was found to be high piezoelectric properties with high Tc (375 °C). To further improve its properties, La_2O_3 was substituted for PbO as an A-site in PYNZ–PT48 [PYNZT-Lax]. The PYNZT-Lax with 0.0 mol% $\leq x \leq$ 3.0 mol% were found that the dielectric permittivity and phase transition temperature exhibited strongly compositional dependence and

its transition range was observed to become broader, indicating typical relaxor ferroelectric behavior. In addition, it was found that the temperature dependence of the inverse relative permittivity of PYNZT-Lax followed a Curie–Weiss Law above the deviation temperature (T_D), providing that there was not a space–charge polarization contribution at high temperatures. Therefore, even if the value of Tc in this study was decreased with the increase in the content of x mol%La_2O_3, its value is still high ($>300\,^{\circ}C$) with high dielectric and piezoelectric properties. It is important for its use in high temperature applications.

References

[1] P. Muralt, Ferroelectric thin films for micro-sensor and actuators: a review, J. Micromech. Microeng. 10 (2000) 136–146.

[2] R.E. Newnham, G.R. Ruschau, Smart electroceramics, J. Am. Ceram. Soc. 74 (1991) 463–480.

[3] E.P. Smirnova, O.V. Rubinshtein, V.A. Isupov, Dielectric and electrostrictive properties of PMN-based complex perovskites, Ferroelectrics 143 (1993) 263–270.

[4] G.A. Smolenskii, A.I. Agranovkaya, Dielectric polarization of a number of complex compounds, Soviet Phys. Solid State 1 (1960) 1429–1437.

[5] H. Ouchi, K. Nagano, S. Hayakawa, Piezoelectric properties of $Pb(Mg_{1/3}Nb_{2/3})O_3$–$PbTiO_3$–$PbZrO_3$ solid solution ceramics, J. Am. Ceram. Soc. 48 (1965) 630–635.

[6] H. Ohuchi, M. Nishida, Phase relation and electric properties of $Pb(Mg_{1/3}Ta_{2/3})O_3$–$PbTiO_3$–$PbZrO_3$ ceramics, J. Jpn. Soc. Powder Powder Metall. 40 (1993) 687–692.

[7] K.V. Im, W.K. Choo, Dielectric properties phase transition of $0.5[(1-x)PbYb_{1/2}Nb_{1/2}O_3$–$xPbTiO_3]$–$0.5PbZrO_3$ solid solution, Jpn. J. Appl. Phys. 36 (1997) 5989–5993.

[8] H. Ohuchi, S. Tsukamoto, M. Ishii, H. Hayakawa, Piezoelectric structural properties of $Pb(Yb_{1/2}Nb_{1/2})O_3$–$PbTiO_3$–$PbZrO_3$ ceramics, J. Euro. Ceram. Soc. 19 (1999) 1191–1195.

[9] K.H. Yoon, Y.S. Lee, H.R. Lee, Effect of $Pb(Yb_{1/2}Nb_{1/2})O_3$ on structural and piezoelectric properties of $Pb(Zr_{0.52}Ti_{0.48})O_3$ ceramics, J. Appl. Phys. 88 (2000) 3596–3600.

[10] K.H. Yoon, H.K. Lee, H.R. Lee, Electromechanical properties of $Pb(Yb_{1/2}Nb_{1/2})O_3$–$PbZrO_3$–$PbTiO_3$ ceramics, J. Am. Ceram. Soc. 85 (2002) 2753–2758.

[11] W.M. Zhu, Z.G. Ye, Ternary $Pb(Yb_{1/2}Nb_{1/2})O_3$–$PbZrO_3$–$PbTiO_3$ system as high-Tc/high-piezoelectric materials, Ceram. Int. 30 (2004) 1443–1448.

[12] S.L. Swartz, T.R. Shrout, Fabrication of perovskite lead magnesium niobate, Mater. Res. Bull. 17 (1982) 1245–1250.

[13] S.B. Krupanidhi, Relaxor type perovskites: primary candidates of nanopolar regions, Proc. Indian Acad. Sci. 115 (2003) 775–788.

[14] A.J. Moulson, J.M. Herbert, Electroceramics: Materials, Properties, Applications, Chapman & Hall, London, 1994, pp. 280–281.

[15] G.A. Smolenskii, Physical phenomena in ferroelectrics with diffuse phase transition, J. Phys. Soc. Jpn. 28 (1970) 26–37.

[16] V. Kirillov, V. Isupov, Relaxation polarization of lead magnoniobate ($PbMg_{1/3}Nb_{2/3}O_3$): ferroelectrics with a diffuse phase transition, Ferroelectrics 5 (1973) 3–9.

[17] K. Uchino, S. Nomura, Critical exponent of the dielectric constants in diffuse phase transition crystals, Ferroelectric Lett. 44 (1982) 55–61.

[18] E. F. Alberta, Relaxor based solid solutions for piezoelectric and electrostrictive applications, Thesis for Ph.D. in Pennsylvania State University, 2003.

[19] M.E. Lines, A.M. Glass, Principles, Applications of Ferroelectrics and Related Materials, Claredon Press Oxford, New York, 1977.

[20] D. Damjanovic, Ferroelectric, dielectric and piezoelectric properties of ferroelectric thin films and ceramics, Rep. Prog. Phys. 61 (1998) 1267–1324.

[21] H. Kungl, T. Fett, S. Wagner, M.J. Hoffmann, Nonlinearity of strain and strain hysteresis in morphotropic LaSr-doped lead zirconate titanate under unipolar cycling with high electric fields, J. Appl. Phys. 101 (2007) 04410/1–04410/8.